AIAA SCITECH 2026 Forum, 12-16 January 2026, Orlando, Florida, Article number 2026-1189
DOI: 10.2514/6.2026-1189

# Turbine-Based Combined Cycle Design and Performance up to Mach 5.0

Zoë A. R. Ashford[1], Vassilios Pachidis[2], and Simon A. Prince[3]
*Centre for Propulsion Engineering, Cranfield University, MK43 0AL, United Kingdom*

**The design of Turbine Based Combined Cycles (TBCCs), consisting of a gas turbine engine and ram- or scramjet, has previously been explored and a number of prototypes have been constructed. The sizing of the TBCC depends heavily on the trajectory flown by the platform, but the definition of the trajectory has been left mainly to optimisation algorithms. This paper presents a methodology that can be used in preliminary engine-airframe sizing studies and explores the impact of some trajectory choices on the performance of a TBCC for three simplified trajectories: constant-EAS climb, climb-dive, and climb-accelerate. It was found that the climb Equivalent Airspeed (EAS), rate of climb, and Top of Climb Mach number all affect the turbojet performance at Mach 2.0; the impact on the ramjet at Mach 5.0 is more noticeable in terms of required intake capture area rather than Specific Fuel Consumption and Specific Net Thrust. When climb-accelerate and climb-dive trajectories are compared to a baseline constant-EAS climb, with the same intake area and Mach 5.0 conditions, trajectories with lower climb EAS (whether climb-dive or climb-accelerate) have improved turbojet performance at Mach 2.0. The qualitative impact of trajectory choices, presented throughout this paper, can inform rudimentary trajectory design with respect to the effect on the engine performance and sizing and, consequentially, on the platform.**

## I. Nomenclature

### Symbols

| | | |
|---|---|---|
| $D$ | = | Drag [kN] |
| $F_N$ | = | Net thrust [kN] |
| $F_{res}$ | = | Resultant force [kN] |
| $g_0$ | = | Acceleration under gravity, 9.8067 [m/s$^2$] |
| $H$ | = | Altitude [m] |
| $L$ | = | Lift [kN] |
| $m$ | = | Mass [kg] |
| $M$ | = | Mach number |
| $\dot{m}$ | = | Mass flow rate [kg/s] |
| $t$ | = | Time [s] |
| $T$ | = | Trajectory duration [s] |
| $V$ | = | True Airspeed [m/s] |
| $V_{EAS}$ | = | Equivalent Airspeed [m/s] |
| $V_v$ | = | Vertical velocity [m/s] |
| $W$ | = | Weight [kN] |
| $\alpha$ | = | Angle of attack [°] |
| $\gamma$ | = | Angle of climb [°] |
| $\gamma_{max}$ | = | Maximum angle of climb [°] |
| $\rho$ | = | Air density [kg/m$^3$] |
| $\rho_0$ | = | Air density at sea level, 1.225 [kg/m$^3$] |
| $\underline{\varsigma}_t$ | = | Trajectory fuel mass fraction |

[1] Researcher, Rolls-Royce University Technology Centre
[2] Professor, Head of Centre for Propulsion and Thermal Power Engineering
[3] Professor in Aerodynamics



Published by AIAA. This is the Author Accepted Manuscript issued with: Creative Commons Attribution License (CC:BY 4.0).
The final published version (version of record) is available online at DOI:10.2514/6.2026-1189. Please refer to any applicable publisher terms of use.

**Subscripts**

| | | |
|---|---|---|
| $_{EOD}$ | = | End of Dive |
| $_{final}$ | = | At end of trajectory |
| $_{fuel}$ | = | Fuel |
| $_{RJ}$ | = | Ramjet |
| $_{TJ}$ | = | Turbojet |
| $_{TOC}$ | = | Top of Climb |
| $_{total}$ | = | For the entire trajectory |

**Acronyms**

| | | |
|---|---|---|
| BPR | = | Bypass Ratio |
| CA | = | Climb-Accelerate |
| CD | = | Climb-Dive |
| deg | = | Degrees |
| EAS | = | Equivalent Airspeed |
| EOD | = | End of Dive |
| FAR | = | Fuel-to-Air Ratio |
| FnSp | = | Specific Net Thrust [kN/kg/s] |
| OPR | = | Overall Pressure Ratio |
| RJ | = | Ramjet |
| SFC | = | Specific Fuel Consumption [g/kN/s] |
| SLS | = | Sea Level Static |
| TAS | = | True Airspeed |
| TBCC | = | Turbine Based Combined Cycle |
| TET | = | Turbine Entry Temperature |
| TJ | = | Turbojet |
| TOC | = | Top of Climb |

## II. Introduction

While hypersonics has long been the domain of rocket propulsion, hypersonic airbreathing propulsion for transatmospheric flight has been explored over the last several decades [1, 2, 3]. Every hypersonic vehicle known to date either uses rocket augmentation or is deployed from a vehicle already travelling at supersonic speeds. However, improvements in gas turbine technology over the last few decades raise the possibility of turbine-based cycles for the subsonic-supersonic range, at which point a ram- or scramjet can be ignited.

With pre-cooling, a gas turbine powerplant can in theory operate up to Mach 5; however, at these speeds, spillage drag may become prohibitive as compressor speed is reduced to avoid overheating [4]. The use of variable components – such as variable area nozzles and inlets, valves to divert excess air around the core, and variable angle compressor blades – permit turbomachinery to operate more efficiently across a wider range. For example, the Pratt & Whitney J-58D engine, which powered the SR-71, could divert air from the fourth-stage compressor into the afterburner to avoid stalling the early compressor stages and choking the later ones; resulting in a > 20% increase in thrust [5, 6]. This variable bypass was effected using valves in bypass ducts, and would come into effect from Mach 2 upwards.

Variable cycle turbofan engines have been used extensively in supersonic airbreathing propulsion: the presence of one or more bypass ducts facilitates the integration of reheat burners, and diverting air through the bypass duct can reduce inlet spillage drag when compressor speed is reduced at higher Mach numbers. The simplest examples have a single fan stage and single bypass; a Variable Area Bypass Injector (VABI) at the rear of the duct to match pressure with the turbine exhaust; and a variable nozzle [7]. The addition of duct burners allows the engine to operate simultaneously in a turbofan and quasi-ramjet mode [8] and could allow a smoother transition between the two for hypersonic application. An afterburner fed by both the bypass duct and turbine exhaust can also act as a "afterramjet" (also known as a "coaxial" ramjet) [9]. Other configurations exist with multiple bypass streams. [10, 7, 11].

In addition to the "coaxial" configuration, a gas turbine engine and ramjet or scramjet combined into a Turbine Based Combined Cycle (TBCC) can retain separate flowpaths downstream of the intake in a "split-flow" or "tandem" TBCC [12]. The advantage of this configuration is that the ramjet can operate as a cold-flowing bypass duct in the subsonic regime, and then be ignited to operate alongside the gas turbine from Mach 1.0 upwards. It was found that while the ramjet had poor efficiency in the lower range, this allowed increasingly more air to be diverted to the ramjet, reducing inlet spillage drag as the turbojet compressor speed was reduced [13]. The split-

flow concept would be the simplest to adapt for a scramjet: the majority of turbo-scramjet concepts have adopted this configuration with a variable geometry ram-duct for dual ramjet-scramjet capability [14].

For a given powerplant configuration, the size and performance of the component cycles depends on the trajectory flown: however, there is no consensus on the optimum flight profile to reach Mach 5.0. The SR-71 mission profile made use of a constant Equivalent Air Speed (EAS) climb in the supersonic regime to Mach 3.4, with a climb-dive manoeuvre in the transonic region [15]. Kepler et al. proposed a climb approximately following a constant dynamic pressure (with EAS around 350 m/s) in the supersonic regime for a Mach 5.0 cruise vehicle, propelled by a hydrogen-fuelled Rocket Based Combined Cycle (RBCC) featuring a Supersonic Through-Flow Fan [16]. However, other research on TBCC-powered Mach 5-capable vehicles have suggested that an optimal climb trajectory would not follow a constant EAS, although in these papers the trajectory is mentioned only in passing and a full justification for the design is not provided [12, 17, 18].

Climb-dive manoeuvres have been investigated by others: for example, Guo et al. proposed an optimised trajectory featuring climb-dives in three distinct low-thrust regions: the transonic regime, turbojet-ramjet transition, and ramjet top-of-climb [19]. While this trajectory was determined as part of a multivariable optimisation, simpler methods are able to recommend the use of climb-dive manoeuvres. For example, the Energy Height method (for minimum fuel or minimum duration of climb) can identify these regions via either graphical or iterative methods [20, 21].

Trajectory design for TBCCs is frequently left as an optimisation exercise, and in many cases the design philosophy is not discussed; the impact of these choices is therefore not determined. This paper presents the qualitative impact of some trajectory choices, alongside a methodology for preliminary engine-airframe sizing studies. These relationships may be used to inform the concept design of platforms with TBCCs up to Mach 5.0.

## III. Methodology

The conceptual study presented in this paper focussed on a Mach 5-capable platform based on the SR-71, powered by a TBCC and flown over a range of trajectories. The modelling comprised three major components: the powerplant (TBCC); the platform; and the trajectory. The engine model contained the validated ramjet and turbojet models; thrust demands to size the models were provided by the trajectory model. The trajectory model contained the calculation procedure for each trajectory type, and when running a particular trajectory relied on engine performance output for each step. To determine the required thrust at each stage of the trajectory, aerodynamic performance data was called from the platform model. All three components were written within the Rolls-Royce version of NASA's Numerical Propulsion System Simulation (NPSS) environment, although each contained detailed performance characteristics which had been generated by external programs.

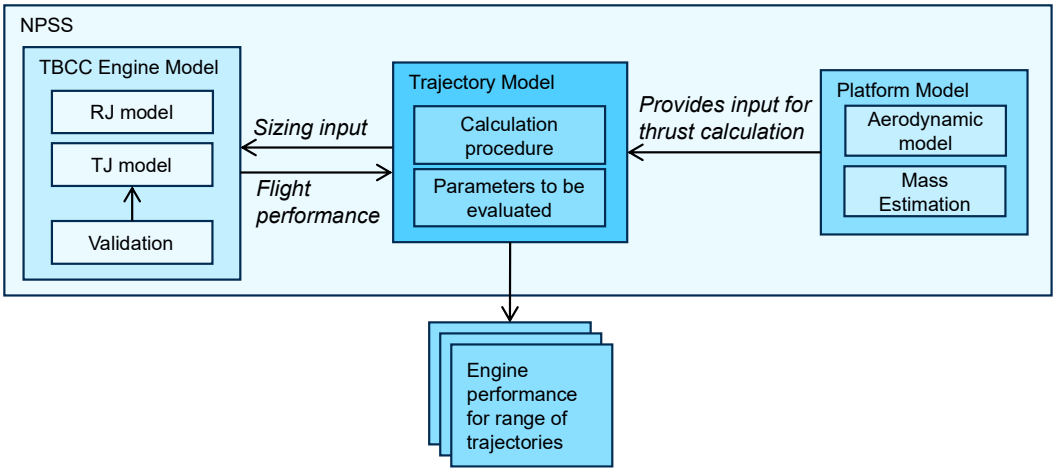



**Figure III-1: Study methodology.**

On the basis of flight heritage, and to limit the number of variables in this investigation, it was decided that the trajectories investigated in this paper would follow a constant EAS in climb. This simplified the trajectories such that the impact of a limited range of parameters that affected powerplant sizing – such as rate of climb and the choice of climb EAS – could be evaluated.

### A. TBCC Model

The baseline TBCC used in this study was a single-spool turbojet in tandem operation with a ramjet; the model structure is shown in Figure III-2. Logic was included in the model to mimic a shared intake for the two powerplants; the flowpaths did not otherwise interact. The baseline TBCC operation was defined as follows:

- Solo gas turbine operation from take-off to Mach 2.0. Ramjet acts as cold-flow non-burning duct.
- Dual ramjet-gas turbine operation from Mach 2.0-3.0. Gas turbine has "priority" over captured air.
- Solo ramjet operation from Mach 3.0-5.0. Gas turbine flowpath assumed to be isolated.

Preliminary modelling indicated that, for the types of trajectories explored, the intake required by the ramjet (determined by its most onerous condition) would always be larger than that required by the turbojet. In the dual-operation regime, the gas turbine specific net thrust (FnSp) was higher than the ramjet: the FnSp for a turbojet and ramjet in an example climb trajectory is shown in Figure III-3. The most fuel-efficient method of distributing air captured by the intake was determined to be for the gas turbine to operate at capacity (controlled by a variable area nozzle) while the ramjet operated with the remaining air captured by the intake. The control of the ramjet nozzle was limited by combustor Mach number, such that if the ramjet combustor Mach number exceeded Mach 0.4 the nozzle would not open further and excess flow captured by the intake would be spilled.

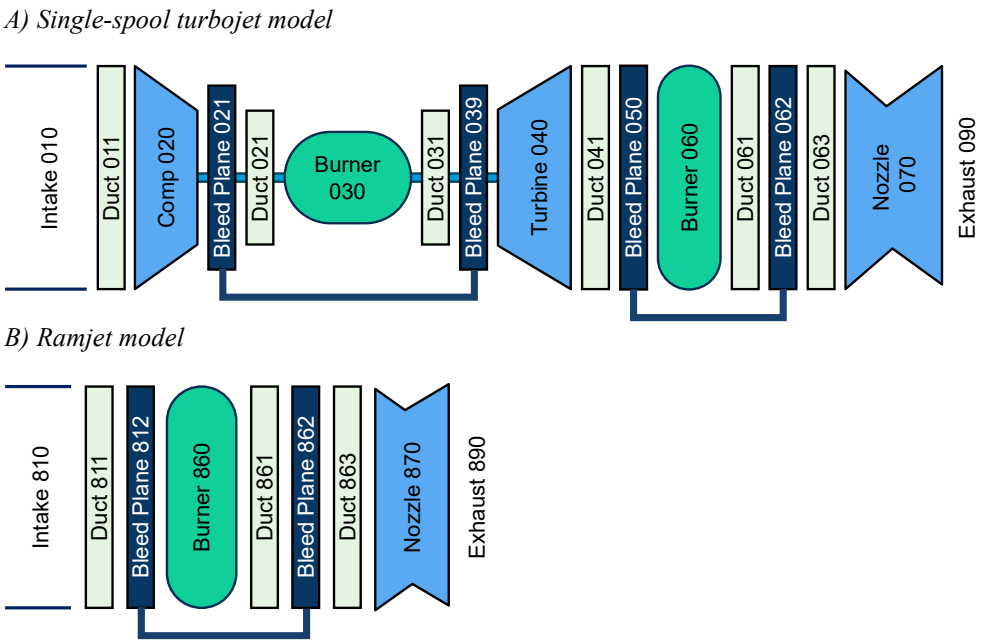



**Figure III-2: Component models of the TBCC model: A) Single-spool turbojet with a turbine cooling bleed and an afterburner cooling jacket bleed. B) Ramjet model with combustor cooling bleed.**

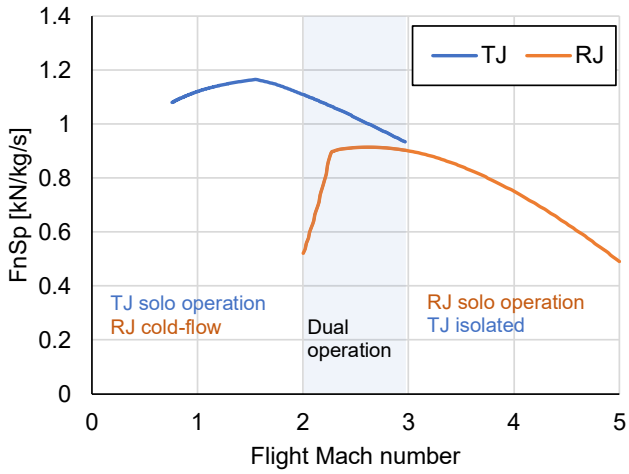



**Figure III-3: Specific Net Thrust, FnSp, for the turbojet (TJ) and ramjet (RJ) powerplants in a climb. The FnSp of the ramjet increases sharply from Mach 2.0-2.3 as the ramjet throttles up to maintain a climb angle.**

The ramjet at its maximum thrust setting was limited to a combustor outlet temperature of 2200 K, Fuel-Air Ratio (FAR) of 0.065 (stoichiometric), and combustor exit Mach number of 0.4. The gas turbine at its maximum thrust setting had a TET of 1400 K and maximum combustor outlet temperature of 900 K, with the afterburner

constrained by the same limits as the ramjet. As the ramjet determined the intake area, the ramjet was sized before the gas turbine so that the impact of the ramduct ram drag on the gas turbine sizing could be determined. Therefore, trajectory decisions that varied the intake area also affected the gas turbine sizing. This sequential modelling was facilitated by the use of two Multiple-Design-Point solvers in series – one for the ramjet, one for the gas turbine – which enabled the ramjet to be sized independently of the gas turbine.

The turbojet model was validated by comparison to existing engine data in a parametric design study. The design point for each cycle was set at Mach 0.87, 12 km, and an off-design case at sea level static (SLS) was calculated. The design of afterburning turbojet and analogous 2-spool turbofan engines was carried out for both dry and afterburning cycles, with TET varying from 1200-1600 K. For the 2-spool engines, the design BPR was varied from 0.2 to 5.0. The overall pressure ratio (OPR) of the 2-spool engines was set to the PR of the single-spool compressor at the design point (51.45), as determined by the intake temperature and the maximum compressor outlet temperature (900 K).

Maximum dry and afterburning engine performance data for some military turbojet engines was collected, including the General Electric (GE) J79 and J85 family, as well as the Pratt & Whitney J58 [22, 23, 24]. By assuming compressor and turbine efficiencies of 0.87, combustor and afterburner efficiencies of 0.95 and 0.80 respectively, and a Fuel Calorific Value of 43 MJ/kg, the specific thrust (FnSp) at sea level was estimated for each engine. The performance data for the models, with afterburner, and existing engines at military thrust is shown in Figure III-4; the performance of the model engines was similar to the existing engines.

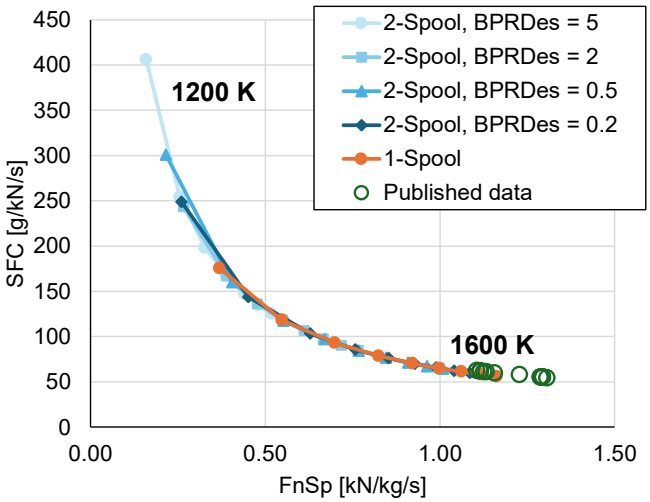



**Figure III-4: Plot of SFC against FnSp for afterburning 1- and 2-spool engines with design TET from 1200 to 1600 K at SLS.**

## B. Platform Definition

The SR-71 was determined to be the most appropriate analogous airbreathing aircraft on which to base the platform aerodynamic performance for this study. Aerodynamic data was estimated for a simplified geometry of the SR-71, using a validated low-fidelity process based on the Pitts-Nielsen-Kaattari method [25]. From this modelling, the maximum lift-to-drag ratio (L/D) was calculated for a range of flight Mach numbers at sea level and at 25 km. These maximum L/D values are shown in Figure III-5.

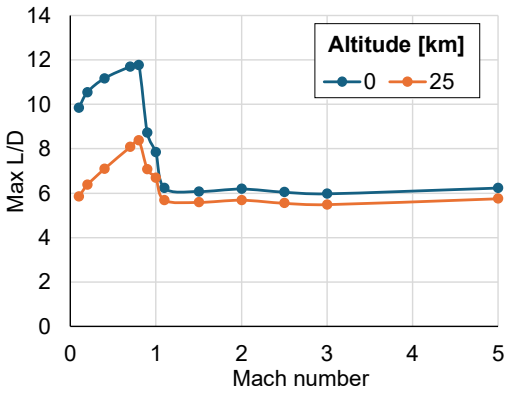



**Figure III-5: Maximum L/D data for an aircraft analogous to the SR-71, with simplified geometry.**

The aircraft was assumed to be a point mass; the sizing mass for the aircraft for each trajectory was set as 35,000 kg and it was assumed that this mass was not affected by engine size. The force-balance diagram on which the following equations was based is shown in Figure III-6.

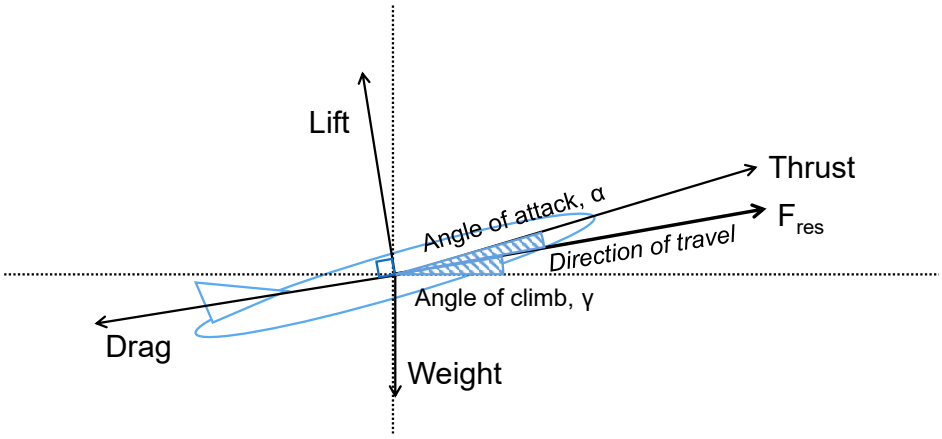



**Figure III-6: Diagram of forces on lifting body in accelerating and climbing flight (not to scale).**

Lift, L, and drag, D, are respectively perpendicular to and collinear with the direction of flight. It was assumed that the net thrust, $F_N$, produced by the propulsion system would be aligned to the longitudinal axis of the aircraft such that the thrust was offset from the direction of travel by the angle of attack, α. The resultant force on the aircraft, $F_{res}$, was assumed to be along the direction of travel, which was itself offset from the horizontal by the angle of climb, γ. Weight is in the vertical direction, downwards.

Resolving the forces parallel and perpendicular to the direction of travel:

$$L + F_N \sin\alpha = W\cos\gamma$$

$$F_{res} = F_N\cos\alpha - D - W\sin\gamma \qquad \textbf{1}$$

As the available aerodynamic characteristics were in terms of L/D, it was efficient to continue with the equations in terms of L/D:

$$\frac{L}{D} = \frac{W\cos\gamma - F_N\sin\alpha}{F_N\cos\alpha - W\sin\gamma - F_{res}} \qquad \textbf{2}$$

Equation **2** could then be rearranged to give an equation for net thrust in terms of L/D:

$$F_N = \frac{W\left(\frac{L}{D}\sin\gamma + \cos\gamma\right) + \frac{L}{D}F_{res}}{\frac{L}{D}\cos\alpha + \sin\alpha} \qquad \textbf{3}$$

$F_{res}$ was expressed in terms of m, the aircraft mass, and dV/dt, the acceleration in terms of the True Airspeed (TAS), V.

$$F_{res} = m\frac{dV}{dt} \quad (4)$$

This led to a final expression for thrust which was then used for trajectory calculations:

$$F_N = \frac{mg_0\left(\frac{L}{D}\sin\gamma + \cos\gamma\right) + \frac{L}{D}m\frac{dV}{dt}}{\frac{L}{D}\cos\alpha + \sin\alpha} \quad (5)$$

These equations were also valid for dive portions of the trajectory using a negative angle of climb, γ.

### C. Trajectory Definition

Three basic trajectory types were explored: a constant-EAS climb; a constant-EAS climb with dive into Mach 5.0 ("climb-dive"); and a constant-EAS climb with a constant-altitude acceleration to reach Mach 5.0 ("climb-accelerate"). Examples of all three types are shown in Figure III-7. The trajectories were modelled in NPSS, using the International Standard Atmosphere atmospheric model [26]. Key evaluation parameters for the trajectories included:

- Trajectory duration, $T_{total}$: time elapsed from start to finish of the modelled trajectory, although this may only represent part of a longer mission profile.
- Trajectory fuel mass fraction, $\varsigma_t$: ratio of the fuel consumed in the trajectory to the aircraft mass at the beginning of the trajectory. As the trajectory may only represent part of the mission profile this is not a true aircraft fuel fraction.
- Intake capture area: The freestream capture area swept out by the intake, which includes any external compression devices.

The trajectories were also evaluated with respect to the TBCC performance.

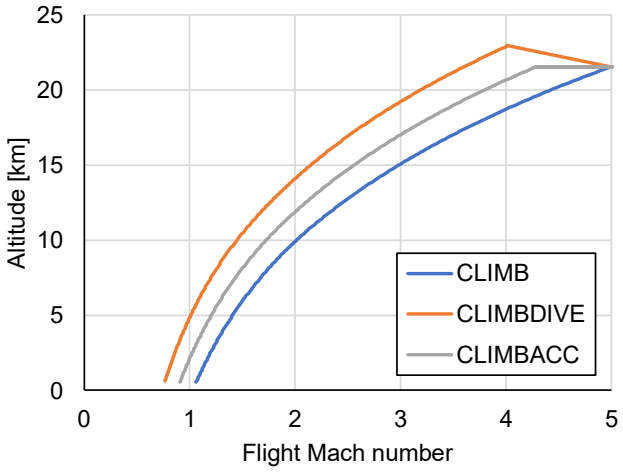



**Figure III-7: Example constant-EAS climb, climb-dive, and climb-accelerate trajectories.**

#### 1. *Constant-EAS Climb*

The simplest trajectory modelled was a constant-EAS climb, analogous to the latter part of the SR-71 trajectory [15]. To eliminate the need for iteration across the whole trajectory, an end-of-climb mass $m_{final}$ was assumed and the calculations were carried out in reverse such that at each step, the mass was increased in accordance with the fuel mass flow rate $\dot{m}_f$ and step duration, Δt.

True airspeed, V, and Equivalent Airspeed, $V_{EAS}$, are related as follows:

$$V = V_{EAS}\sqrt{\frac{\rho_0}{\rho}} \quad (6)$$

Where ρ and $\rho_0$ are the atmospheric density at some point in the trajectory and at sea level, respectively. Therefore, for a constant-EAS trajectory, the altitude H and velocity V are linked and for a given altitude step dH the associated change in velocity, dV could be found. The acceleration term in the thrust equation was broken down as follows:

$$\frac{dV}{dt} = \frac{dH}{dt} \times \frac{dV}{dH} \quad \textbf{7}$$

The $\frac{dH}{dt}$ term could then be further decomposed -

$$\frac{dH}{dt} = V_v = V \sin\gamma \quad \textbf{8}$$

$$\frac{dV}{dt} = \frac{dV}{dH} V \sin\gamma \quad \textbf{9}$$

The thrust equation was then expressed as follows:

$$F_N = \frac{mg_0\left(\frac{L}{D}\sin\gamma + \cos\gamma\right) + \frac{L}{D} m \frac{dV}{dH} V \sin\gamma}{\frac{L}{D}\cos\alpha + \sin\alpha} \quad \textbf{10}$$

From these equations for a constant-EAS trajectory with a given altitude step size, the necessary acceleration (and hence thrust) for a given angle of climb could be approximated. However, it was assumed that a maximum-thrust trajectory would be the most efficient in terms of fuel consumption and time. Therefore for each point in the trajectory, the engine performance at its maximum thrust power-setting was determined and the maximum possible angle of climb $\gamma$ at that point calculated to determine the altitude, velocity, and mass of the platform for the next step.

A maximum allowable $\gamma$ was defined. If this value was exceeded during the climb – i.e. if the calculated maximum possible $\gamma$ was greater than this $\gamma_{max}$ value – the thrust was instead calculated with $\gamma_{max}$ and this demand sent to the engine model. The altitude, velocity, and platform mass were updated accordingly.

Preliminary modelling indicated that both the TOC angle of climb and Mach number had a significant impact on fuel consumption and engine sizing, thus a range of both parameters were evaluated.

*2. Constant-EAS Climb with Dive*

The climb-dive trajectory assumed a constant-EAS climb to some Mach number $M_{TOC}$, with some TOC angle of climb $\gamma_{TOC}$, followed by a dive to Mach 5 with some End-of-Dive (EOD) angle of dive $\gamma_{EOD}$. The End-of-Dive (EOD) EAS was taken as 350 m/s (the highest dynamic pressure featured in Guo et al. [19]). As with the constant-EAS climb, the climb-dive trajectory was initialised at the end of the trajectory (end of dive) and calculated backwards.

To simplify and expedite the modelling, it was desirable to avoid iteration across multiple steps of the trajectory: this was a disadvantage for the dive, as $\frac{dV}{dH}$ was no longer fixed by a constant EAS. However, to ensure that the correct TOC conditions were reached, an average $\frac{dV}{dH}$ was calculated:

$$\left(\frac{dV}{dH}\right)_{average} = \frac{V_{EOD} - V_{TOC}}{H_{EOD} - H_{TOC}} \quad \textbf{11}$$

For each step of the dive and with the maximum thrust output by the engine, the angle of dive $\gamma_{EOD}$ was iterated until the $\frac{dV}{dH}$ component of the thrust equation was equal to the average value for the dive.

Evidently, such a climb-dive trajectory has both the TOC and EOD as critical sizing conditions. For a given climb EAS, a range of TOC Mach numbers and EOD angles of dive were explored. Where a combination of $\gamma_{EOD}$ and $M_{TOC}$ resulted in an undersized powerplant for TOC (i.e. climb could not be sustained in those conditions) the case was flagged and removed from the set.

*3. Constant-EAS Climb with Constant-Altitude Acceleration*

The climb-accelerate trajectory assumed a constant-EAS climb until the altitude determined by the Mach 5.0 condition was achieved, after which the platform accelerated at maximum thrust to Mach 5.0. In this case, it was found that the TOC conditions would typically be more onerous than the acceleration (with no vertical component to the velocity, the excess thrust required for acceleration was much lower than in climb). Therefore, the platform was sized for and initialised at TOC; the trajectory was then calculated forwards in time as the platform accelerated at maximum thrust to Mach 5.0 (using the thrust equation as described in Equation **5**). Once the Mach 5.0 condition had been reached, the model reverted the platform conditions to TOC and the climb portion was calculated in reverse as previously described.

*4. Trajectory Comparison Study*

To facilitate the comparison of the performance of the platform with respect to the three trajectory types, a baseline climb trajectory at 350 m/s EAS and 2° $\gamma_{TOC}$ was defined. Climb-dive and climb-accelerate trajectories were then found with same intake area and same final Mach 5 condition by varying $M_{TOC}$ and $\gamma_{EOD}$ (climb-dive), and climb EAS and $\gamma_{TOC}$ (climb-accelerate), respectively.

## IV. Results and Discussion

### A. Constant-EAS Climb

Trajectories with EAS from 200 to 350 m/s were evaluated with $\gamma_{TOC}$ from 0.5-3.0 degrees. The impact of these parameters on intake area and trajectory duration is shown in Figure IV-1. Higher climb EAS, reducing the altitude and thus increasing air density for a given Mach number condition, reduced the intake area requirement. Lower $\gamma_{TOC}$ reduced the TOC thrust demand and thus also reduced the intake area. Trajectory duration, by contrast, showed little variance with climb EAS and but was increased with greater $\gamma_{TOC}$; this is to be expected, as it would take longer to gain altitude with a shallower climb angle.

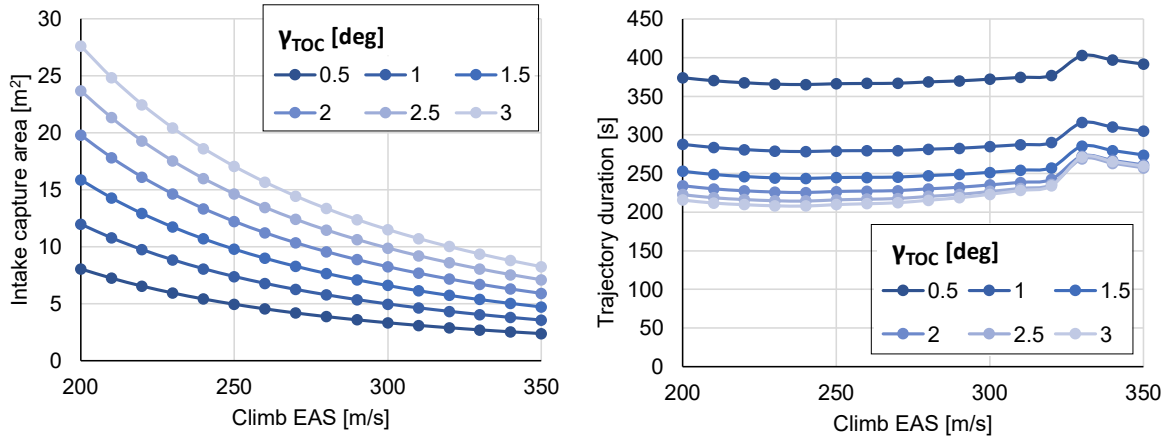



**Figure IV-1.** ***Left:*** **Intake area as a function of both climb Equivalent Airspeed (EAS) and Top-of-Climb angle of climb ($\gamma_{TOC}$).** ***Right:*** **Trajectory duration as a function of both climb EAS and $\gamma_{TOC}$.**

The step in the trajectory duration values was determined to be an artefact of the atmospheric model. The gas turbine model was sized at Mach 2.0 for the trajectory EAS, and the altitude at Mach 2.0 between 320 and 330 m/s traverses 11 km – the location of the troposphere-tropopause transition in ISA, shown in Figure IV-2. Figure IV-3 shows the net thrust, $F_N$, calculated for a range of EAS at Mach 1.8 and Mach 2.0. For both Mach numbers, there was a discontinuity in $F_N$ around 11 km altitude: the change in temperature gradients reduced the calculated thrust demand below 11 km by 10%. This also reduced the turbojet engine size, increasing air available to the ramjet in the dual-operation regime and ultimately increasing total fuel consumption.

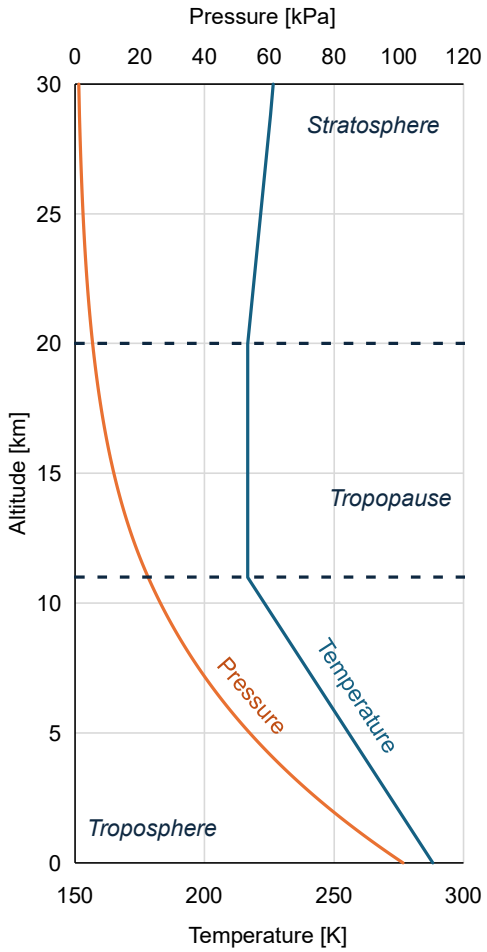



**Figure IV-2: Values of pressure and temperature with altitude according to the International Standard Atmosphere model [26].**

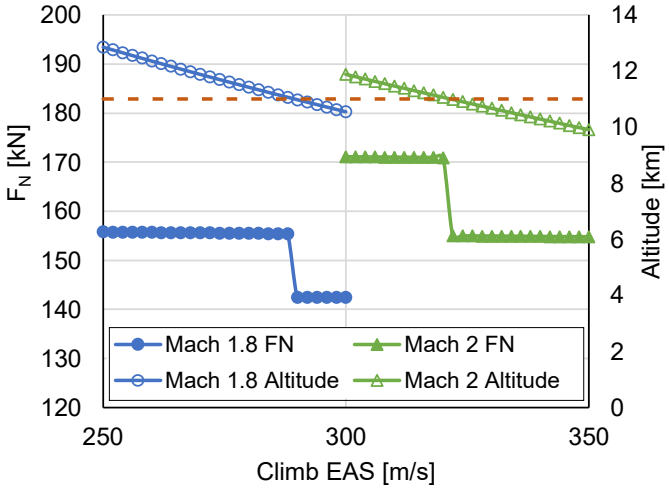



**Figure IV-3: Net thrust, $F_N$, for 5 degree climb and altitude at Mach 1.8 and 2.0, for a range of climb EAS. For both Mach numbers, there is a step change in the thrust at 11 km.**

The impact of $\gamma_{TOC}$ and climb EAS on engine performance in a constant-EAS climb are shown in Figure IV-4, for the sizing conditions for both powerplants: the turbojet at its maximum solo operating point (Mach 2.0) and the ramjet at its maximum operating point (Mach 5.0). It was evident that the climb EAS had minimal effect on either parameter, whereas $\gamma_{TOC}$ impacted both the Specific Fuel Consumption, SFC, and specific net thrust, FnSp. A larger $\gamma_{TOC}$ demanded a larger intake area for the required TOC thrust, which increased the ram drag produced

at the turbojet sizing condition: this resulted in a larger turbojet to compensate, but more fuel was therefore required (increasing SFC) and much of the captured air was "wasted" in the cold-flow ramduct (decreasing FnSp). Conversely, the variation in SFC and FnSp for the ramjet at Mach 5.0 was entirely due to the change in climb EAS and thus TOC altitude: for EAS of 200-350 m/s, Mach 5.0 is reached in the stratosphere. The lower altitude at Mach 5.0 for a higher EAS means that the freestream air temperature is lower, and so more heat addition could occur in the combustor – ultimately decreasing SFC and increasing FnSp.

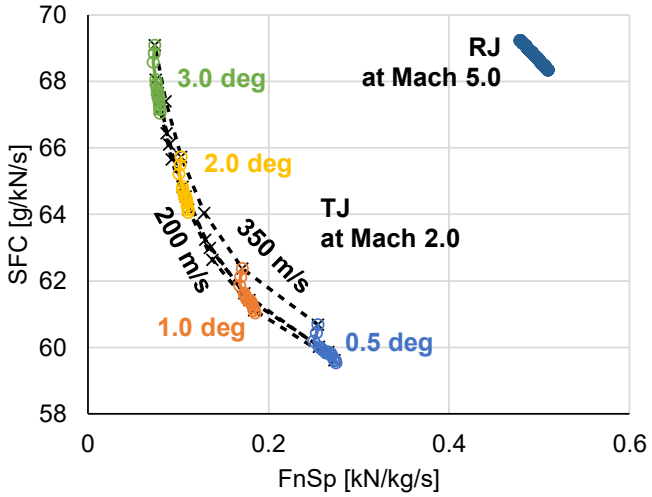



**Figure IV-4: Relationship between Specific Net Thrust, FnSp, and Specific Fuel Consumption, SFC, for the turbojet powerplant at Mach 2.0 and the ramjet at Mach 5.0 for a range of $\gamma_{TOC}$ and climb EAS.**

The relationship between FnSp and SFC shown in Figure IV-4 is analogous to that presented in the validation exercise for the afterburning 1 and 2-spool engines (Figure III-4): while this trajectory model only considered a 1-spool turbojet, the ramduct is similar to a bypass duct. Powerplants sized for greater $\gamma_{TOC}$ had a larger effective bypass duct, and the impact of $\gamma_{TOC}$ on SFC and FnSp was similar the impact of BPR seen in Figure III-4.

### B. Constant-EAS Climb with Dive

Trajectories with TOC Mach numbers from 3.7 to 4.5 and $\gamma_{EOD}$ from -0.1 to -3.0 degrees were evaluated. The climb EAS was 250 m/s and EOD EAS was 350 m/s. It was discovered that not all $\gamma_{EOD}$ values sized an engine that could sustain a climb at all TOC Mach numbers.

The impact of $\gamma_{EOD}$ and the TOC Mach number on the intake area is shown in Figure IV-5. Intake area increased with $\gamma_{EOD}$, as EOD was the ramjet sizing condition and a steeper dive required greater thrust. The decrease in intake area size with larger TOC Mach number is counterintuitive. However, Table IV-1 demonstrates that a dive starting from Mach 3.7 at 250 m/s EAS had a much greater change in velocity with altitude (dV/dH) to Mach 5.0, at 350 m/s EAS, than a dive starting at Mach 4.5. As the powerplant was sized using the average dV/dH for the dive, a dV/dH value of greater magnitude would require a more powerful engine, and the trend in dV/dH with Mach number shown in Figure IV-6 is coherent with the increased intake area shown in Figure IV-5.

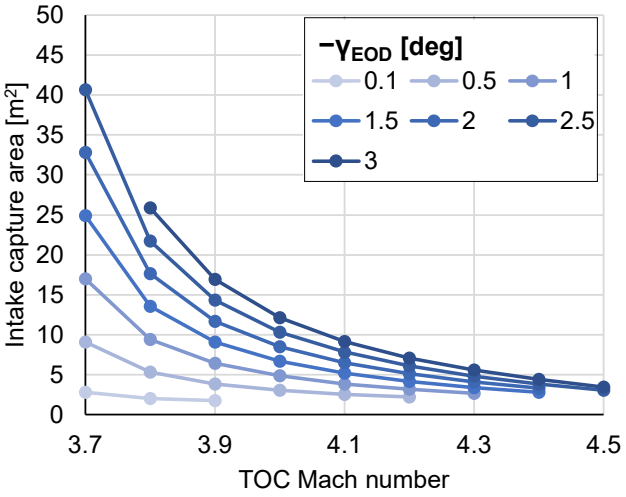



**Figure IV-5: Intake area for a range of EOD angles of dive (-$\gamma_{EOD}$) and TOC Mach numbers.**

**Table IV-1: Velocities and altitudes for two example TOC Mach numbers and for EOD at Mach 5.0**

| | TOC | | EOD |
|---|---|---|---|
| Mach no. | 3.7 | 4.5 | 5.0 |
| EAS [m/s] | 250 | 250 | 350 |
| TAS [m/s] | 1090 | 1340 | 1480 |
| Altitude [km] | 22.0 | 24.5 | 21.6 |

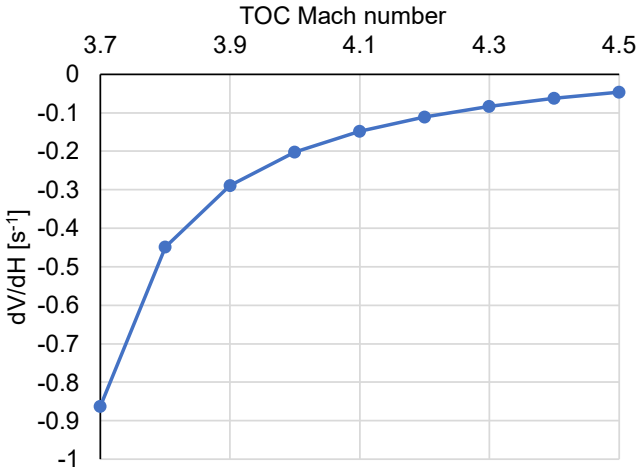



**Figure IV-6: Change in velocity with altitude for dives from various TOC Mach numbers at 250 m/s EAS to Mach 5.0 at 350 m/s EAS.**

The trajectory duration and fuel mass fraction, $\varsigma_t$, with respect to the EOD dive angle -$\gamma_{EOD}$ and TOC Mach number are shown in Figure IV-7. The trajectory duration was approximately inversely proportional to the intake area: a larger engine achieved the climb more rapidly, and increasing the magnitude of $\gamma_{EOD}$ and lowering the TOC Mach number both increased engine size. The trend in fuel consumption partially correlated with trajectory duration, with the exception of the engines with the largest intake areas (Mach 3.7-3.9, -$\gamma_{EOD}$ = 1.5-3.0) for which the ram drag of the ramduct in the gas turbine solo-operation regime had a significant impact on the gas turbine sizing. The decoupling of the intake size from the platform aerodynamics means that the results presented here may neglect key aerodynamic effects, but qualitative relationships can still be derived.

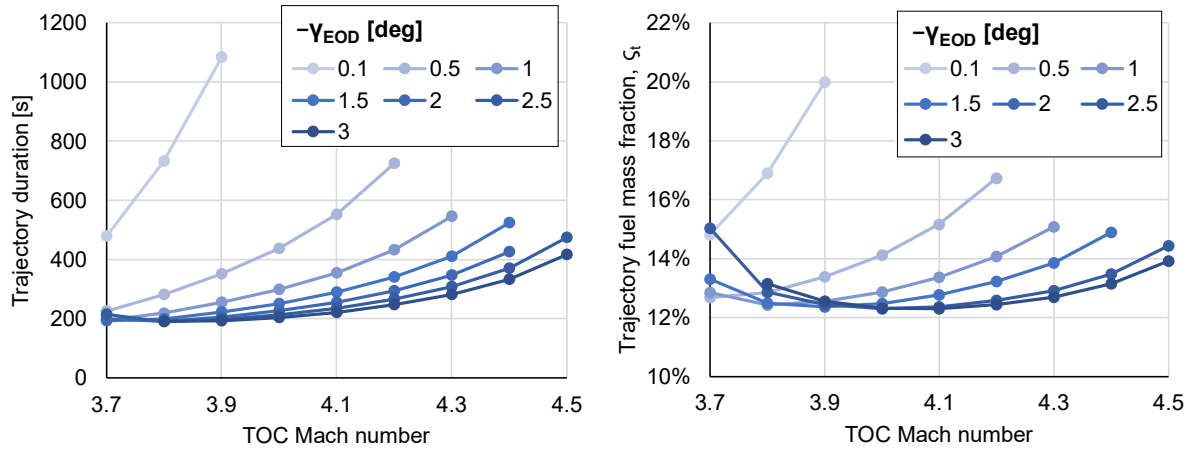



**Figure IV-7: *Left:* Trajectory duration in terms of TOC Mach number and EOD angle of dive, - $\gamma_{EOD}$. *Right*: Trajectory fuel mass fraction, $\varsigma_t$, in terms of TOC Mach number and - $\gamma_{EOD}$.**

The minimum EOD angle of dive ($-\gamma_{EOD}$) for each TOC Mach number was defined by the smallest powerplant that was able to sustain the climb and dive. Cases where the powerplant was unable to sustain the climb or dive were removed from the set. The minimum $-\gamma_{EOD}$ values increased with TOC Mach number: a higher Mach number at TOC increased the thrust demand and thus smaller $-\gamma_{EOD}$ values resulted in a powerplant too small to sustain climb at TOC. Further climb-dive trajectories were calculated for a climb EAS of 270 m/s. The minimum Mach number was limited by altitude and so the range of Mach numbers was reduced to 4.0-4.5. The minimum $-\gamma_{EOD}$ to allow climb for both EAS values, are shown in Figure IV-8.

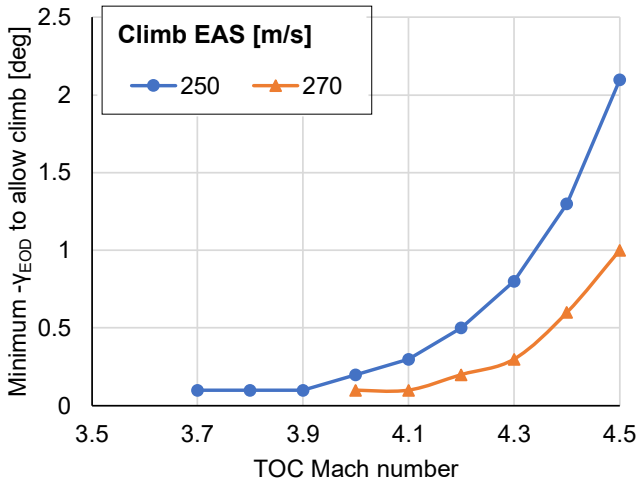



**Figure IV-8: Minimum $-\gamma_{EOD}$ required for powerplant to be able to sustain climb at a given TOC Mach number, for climb EAS of 250 and 270 m/s.**

The impact of EOD angle of dive, $-\gamma_{EOD}$, and TOC Mach number on engine performance in the climb-dive trajectory is shown in Figure IV-9, for the sizing conditions for both powerplants: the turbojet at its maximum solo operating point (Mach 2.0) and the ramjet at its maximum operating point (Mach 5.0, 350 m/s EAS). Clearly, both $\gamma_{EOD}$ and TOC Mach number impacted both the Specific Fuel Consumption, SFC, and specific net thrust, FnSp. Both larger $-\gamma_{EOD}$ and lower TOC Mach number demanded a larger intake area for the required EOD thrust (for a more onerous climb, and for a greater dV/dH, respectively). The larger intake and ramduct increased ram drag at the turbojet sizing condition, and thus turbojet size; necessitating more fuel (increasing SFC) and much of the captured air was "wasted" in the cold-flow ramduct (decreasing FnSp). As the Mach 5.0 condition for each case was at the same EAS (350 m/s), the performance of the ramjet at Mach 5.0 did not vary.

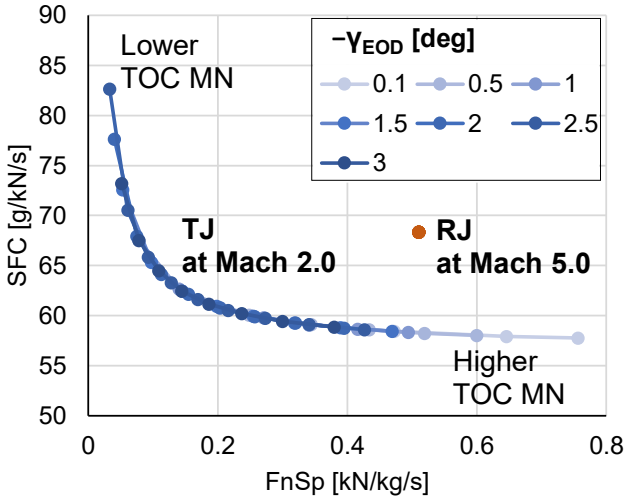



**Figure IV-9: Relationship between Specific Net Thrust, FnSp, and Specific Fuel Consumption, SFC, for the turbojet powerplant at Mach 2.0 and the ramjet at Mach 5.0 for a range of -$\gamma_{EOD}$ and TOC Mach number (MN).**

The relationship between FnSp and SFC shown in Figure IV-9 is analogous to that presented in the validation exercise for the afterburning 1 and 2-spool engines (Figure III-4): where the ramduct becomes a bypass duct to the 1-spool turbojet. Powerplants for more onerous EOD conditions had a larger effective bypass duct, and the impact of -$\gamma_{EOD}$ and TOC Mach number on SFC and FnSp was similar the impact of BPR seen in Figure III-4.

### C. Constant-EAS Climb with Constant-Altitude Acceleration

Climb-accelerate trajectories with climb EAS of 250-350 m/s and $\gamma_{TOC}$ from 0.5-5.0 were evaluated. Each trajectory followed a constant-EAS climb to an altitude of 21560 m after which the platform accelerated at constant altitude to Mach 5.0 (with EAS of 350 m/s).

Analogous to the constant-EAS climb trajectories, a "step" was observed in the whole-trajectory data (e.g. fuel consumption and trajectory duration - Figure IV-10) between the trajectories with 320 and 325 m/s EAS. At and below 320 m/s EAS, the altitude at the gas turbine sizing point (Mach 2.0) was above 11 km, and at and above 325 m/s EAS the altitude of the gas turbine sizing point was below 11 km. Due to a difference in the temperature gradient either side of 11 km, the thrusts calculated for Mach 2.0 below 11 km altitude were lower than those above 11 km by around 10%. The proportion of total trajectory fuel consumed by the gas turbine was found to be greater for these lower-altitude, higher-EAS cases, indicating that the increase in both trajectory time and fuel consumption was primarily due to a slower climb from the gas turbine.

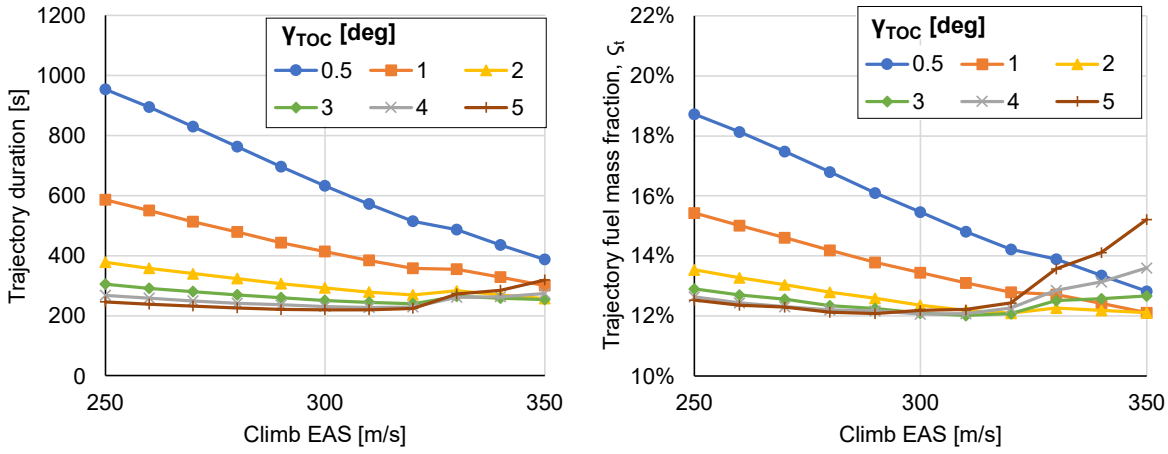



**Figure IV-10. *Left:* Total trajectory duration as a function of both climb EAS and TOC angle of climb, $\gamma_{TOC}$. *Right:* Trajectory fuel mass fraction, $\zeta_t$, as a function of both climb EAS and $\gamma_{TOC}$.**

The impact of the gas turbine is demonstrated in Figure IV-11. Ramjet powerplants sized for higher TOC $\gamma_{TOC}$ were larger and had lower trajectory durations for similar aircraft mass. As the gas turbine sizing point was at a constant Mach number and $\gamma$ there was little variation in the thrust (with the exception of the troposphere-tropopause transition), therefore platforms designed for higher $\gamma_{TOC}$ spent a greater proportion of the trajectory duration powered by the gas turbine. In addition, larger intake areas demanded by the ramjet created more ram drag – this reduced the net thrust produced by the TBCC in turbojet-only mode and explains the increased trajectory duration and fuel consumption of the gas turbine. According to the model intake logic, the smaller gas turbine powerplants would allow more air to be ingested by the ramjet in dual-operation mode; in this range the specific net thrust of the ramjet was lower than the gas turbine and so the climb rate from the overall powerplant at e.g. 320 m/s was reduced compared one sized at 325 m/s. Therefore, the higher $\gamma_{TOC}$ trajectories were impacted to a greater extent by the change in gas turbine sizing condition.

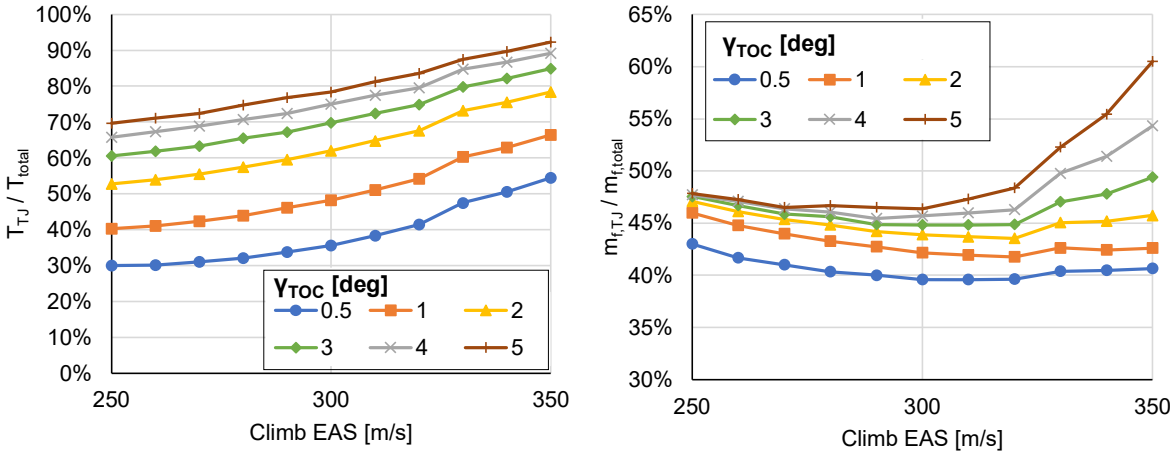



**Figure IV-11. *Left:* Proportion of trajectory duration with the turbojet powerplant active ($T_{TJ}/T_{total}$), as a function of both climb EAS and $\gamma_{TOC}$. *Right:* Proportion of total trajectory fuel consumed by TJ ($m_{f,TJ}/m_{f,total}$), as a function of both climb EAS and $\gamma_{TOC}$.**

Contrary to the constant-EAS climb results, the intake area increased with climb EAS (although a similar decrease in intake area with lower $\gamma_{TOC}$ was still observed). This increase was due to the changing TOC Mach number: as the TOC altitude was fixed in accordance with the Mach 5.0 condition, increasing climb EAS increased the TOC Mach number and thus the TOC thrust requirement for the powerplant.

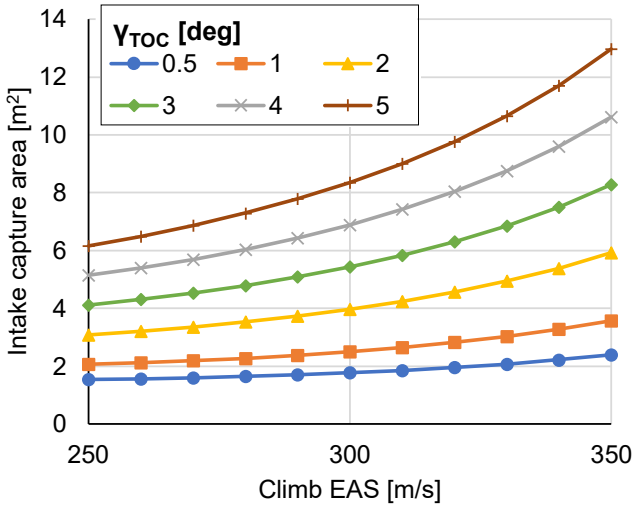



**Figure IV-12: Intake area sized for a range of climb EAS and $\gamma_{TOC}$.**

The impact of $\gamma_{TOC}$ and climb EAS on engine performance for the climb-accelerate trajectory is shown in Figure IV-13, for the sizing conditions for both powerplants: the turbojet at its maximum solo operating point (Mach 2.0) and the ramjet at its maximum operating point (Mach 5.0, 350 m/s EAS). Both larger $\gamma_{TOC}$ and larger climb EAS constituted more onerous TOC conditions: for a fixed altitude, TOC was reached at a larger Mach

number for increased climb EAS. Increasing $\gamma_{TOC}$ and climb EAS therefore necessitated a larger intake area to achieve the TOC thrust. As previously discussed, the larger intake and ramduct increased ram drag at the turbojet sizing condition, increasing turbojet size and thus fuel consumption (increasing SFC). However as the ramduct area increased ahead of the turbojet size, a large proportion of the captured air was effectively bypassed via the ramduct, decreasing FnSp. The relationship between SFC and FnSp with more onerous TOC conditions (higher $\gamma_{TOC}$ and climb EAS) is therefore analogous to the impact of a higher BPR for afterburning 2-spool engines, as seen in Figure III-4.

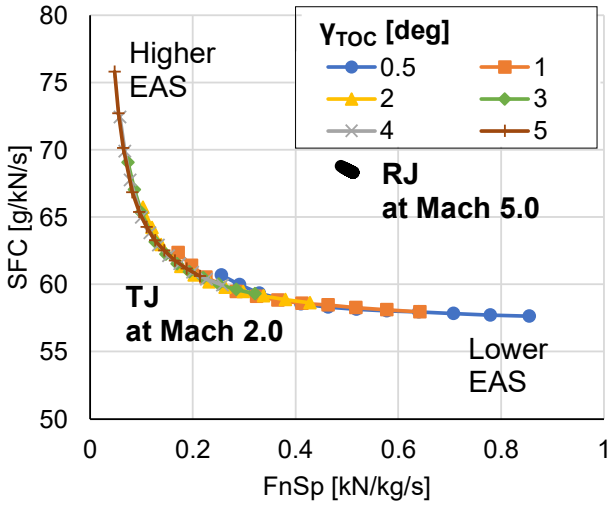



**Figure IV-13: Relationship between Specific Net Thrust, FnSp, and Specific Fuel Consumption, SFC, for the turbojet powerplant at Mach 2.0 and the ramjet at Mach 5.0 for a range of $\gamma_{TOC}$ and climb EAS.**

For the climb-accelerate trajectories, the ramjet was sized for TOC, at varying Mach numbers. However, as TOC altitude was fixed in the stratosphere (at 21560 m in accordance with the Mach 5.0 condition) there was minimal impact of $\gamma_{TOC}$ and climb EAS on SFC or FnSp.

## D. Trajectory Comparison Study

A baseline constant-EAS climb was defined with 350 m/s climb EAS and TOC $\gamma_{TOC}$ of 2 degrees. Climb-dive and climb-accelerate trajectories were then found with the same Mach 5.0 condition and same intake area, 5.925 $m^2$. The climb-accelerate trajectories had climb EAS from 250-350 m/s, and for each EAS, $\gamma_{TOC}$ was varied to match intake area. The climb-dive trajectories had climb EAS of 250-290 m/s and TOC Mach numbers from 3.7-4.5, and $-\gamma_{EOD}$ was varied to match the intake area. A comparison of the SFC and FnSp for all three trajectory types is shown in Figure IV-14.

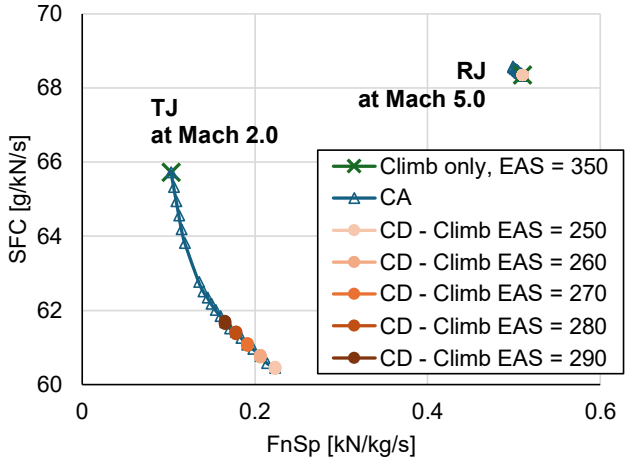



**Figure IV-14: Comparison of SFC and FnSp for: the baseline constant-EAS climb ("Climb only"); climb-accelerate ("CA") trajectories at a range of TOC Mach numbers; and climb-dive ("CD") trajectories with**

**a range of TOC Mach numbers and -$\gamma_{EOD}$; all with the same intake area and same Mach 5.0 EAS of 350 m/s.**

As seen for the individual trajectory types, there was negligible difference in ramjet performance at TOC: the only variation came from the climb-accelerate cases where the ramjet sizing was carried out at TOC (at or below Mach 5.0), in contrast to the climb-dive and climb trajectories where ramjet sizing always occurred at Mach 5.0. However, the turbojet performance at Mach 2.0 clearly improved with reduction in climb EAS. The clustering of the climb-dive cases for each climb EAS indicated that the performance impact of TOC Mach number and $\gamma_{EOD}$ "cancelled out" for the same intake area.

The impact on trajectory duration and $\varsigma_t$, shown in Figure IV-15, was minor: a climb-dive trajectory with climb EAS of 250 m/s was only around 35 s slower than the most expedient climb-accelerate trajectory. Similarly, the maximum fuel consumption of any of the climb-dive trajectories was only 1.2 % greater than the constant-EAS climb.

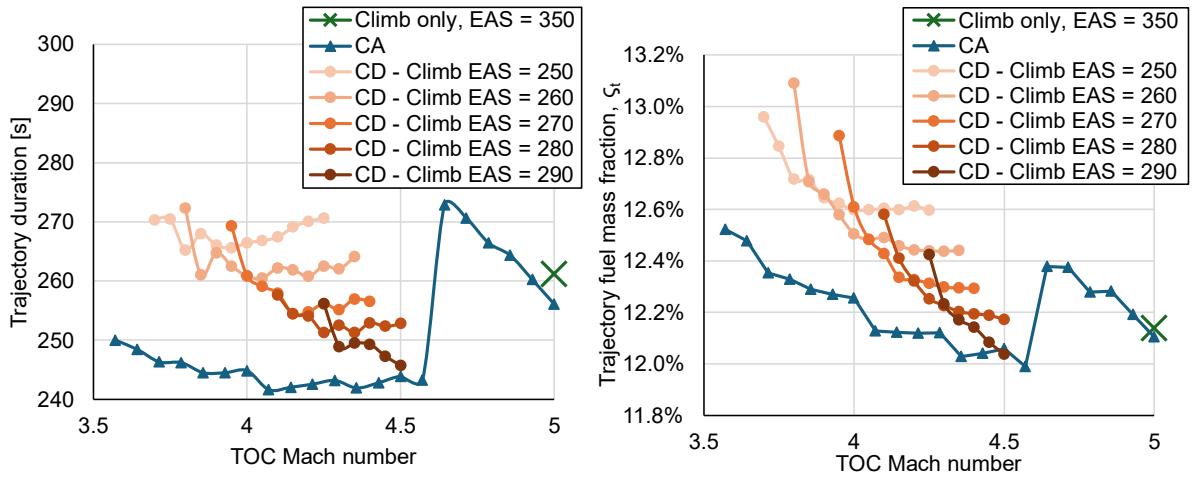



**Figure IV-15. *Left:* Total trajectory duration, and *Right*: Trajectory fuel mass fraction, $\varsigma_t$, for: the baseline constant-EAS climb ("Climb only"); climb-accelerate ("CA") trajectories at a range of TOC Mach numbers; and climb-dive ("CD") trajectories with a range of TOC Mach numbers and -$\gamma_{EOD}$; all with the same intake area and same Mach 5.0 EAS of 350 m/s.**

Therefore, for the given intake area constraint, a climb-dive or climb-accelerate trajectory with a lower climb EAS provided the most performance benefit to the propulsion system, compared to a direct climb.

## V. Summary and Conclusions

The design of TBCCs has been explored previously (e.g. [19, 3]) but the trajectory design and its impact on the powerplant design and performance are frequently left as an optimisation exercise. This paper presented the effect of various trajectory choices on three simple trajectory types: climb, climb-dive, and climb-accelerate.

For constant-EAS climb trajectories, engine performance at Mach 2.0 was optimal at lower $\gamma_{TOC}$, and increasing climb EAS minimised the intake area; there was little impact from either parameter on the ramjet TOC performance. For the climb-dive trajectories, a shallower dive (lower -$\gamma_{EOD}$) and higher TOC Mach number reduced SFC and increased FnSp; both parameters also reduced the required intake capture area. However, the decrease in intake area with higher TOC Mach number was found to be proportional to the average dV/dH calculated for the dive. As a constant, averaged dV/dH assumption was made for the dive, a future study should investigate the dive using an iterative approach to ensure the intake area-Mach number relationship is not an artefact of this assumption. For the climb-accelerate trajectories, turbojet performance at Mach 2.0 was improved with lower EAS and $\gamma_{TOC}$. The performance of the ramjet at Mach 5.0 was not significantly affected, but the intake area increased with higher climb EAS and $\gamma_{TOC}$. Therefore, the design of a climb-accelerate trajectory must include a trade-off for the climb EAS, to minimise the intake area demanded by the ramjet at TOC while maintaining the required turbojet performance.

When climb-accelerate and climb-dive trajectories were compared to a baseline constant-EAS climb, with the same intake area and Mach 5.0 conditions, it was found that trajectories with lower climb EAS (whether climb-dive or climb-accelerate) provided improved engine performance at Mach 2.0 in terms of SFC and FnSp. These trajectories with lower climb EAS tended to have longer overall trajectory duration and higher trajectory mass fuel fraction, $\varsigma_t$. However, the total range in trajectory duration was 35 s and in $\varsigma_t$, 1.2%: the impact is minor and may be ignored if a designer's priority is engine performance.

The ramjet design conditions and thrust demand consistently required a larger intake area than the turbojet; the ramjet therefore had the most impact on the overall powerplant sizing. The ramjet, which acted as a cold-flowing bypass duct below Mach 2.0, then affected the turbojet sizing and performance even when the flight conditions for the turbojet were unchanged. The change in turbojet design thrust across the troposphere-tropopause boundary demonstrated that varying the turbojet design flight conditions – and thus design thrust – would impact the overall powerplant performance. However, this effect appeared to be minor and the choice of turbojet design point would most likely be influenced by thermal limits for a given turbojet engine.

To the best of the authors' knowledge, this paper presents for the first time a methodology that can be used in preliminary engine-airframe sizing studies, for three simplified trajectories: constant-EAS climb, climb-dive, and climb-accelerate. The qualitative impact of trajectory choices, presented throughout this paper, can inform rudimentary trajectory design with respect to the effect on the engine performance and sizing and, consequentially, on the platform.

## Acknowledgments

The authors wish to thank Richard Tunstall and Martin Goodhand of Rolls-Royce for their support and contributions to this research.

## References

[1] H. Kobayashi, T. Sato, H. Taguchi, K. Fujita, S. Sawai, N. Tanatsugu, T. Kojima, K. Okai and Y. Maru, "Development status of Mach 6 turbojet engine in JAXA," in *International Astronautical Federation - 55th International Astronautical Congress*, 2004.

[2] L. Serre and S. Defoort, "Lapcat II: Towards a Mach 8 civil aircraft concept, using advanced Rocket/Dual-mode ramjet propulsion system," in *16th AIAA/DLR/DGLR International Space Planes and Hypersonic Systems and Technologies Conference*, 2009.

[3] M. Ito, "International collaboration in super/hypersonic propulsion system research project (HYPR)," *Aeronautical Journal,* vol. 104, no. 1040, pp. 445-451, 2000.

[4] T. Powell and M. Glickstein, "Precooled turbojet engine cycle for high Mach number applications," in *AIAA/SAE/ASME/ASEE 24th Joint Propulsion Conference*, 1988.

[5] J. Connors, "Higher and Faster," in *The Engines of Pratt & Whitney: A Technical History: As Told by the Engineers Who Made the History*, Reston ,VA, American Institute of Aeronautics and Astronautics, 2010, pp. 319-339.

[6] Blackbird Historian, "The J-58 Engine," 27 January 2023. [Online]. Available: https://www.thesr71blackbird.com/Aircraft/Engines/j58-the-powerplant-for-the-blackbirds.

[7] R. D. Allan, "GENERAL ELECTRIC COMPANY VARIABLE CYCLE ENGINE TECHNOLOGY DEMONSTRATOR PROGRAM," in *AlAA SAE ASME 15TH JOINT PROPULSION CONFERENCE*, 1979.

[8] R. A. Howlett, J. Johnson, J. Sabatella and T. Sewall, "CR-135148: Advanced Supersonic Propulsion Study Phase 3 Final Report," NASA, 1976.

[9] G. Champagne, "Payoffs for supersonic through flow fan engines in high Mach transports and fighters," in *AIAA/ASME/SAE/ASEE 24th JOINT PROPULSION CONFERENCE*, 1988.

[10] R. Brown, "Integration of a variable cycle engine concept in a supersonic cruise aircraft," in *AIAA/SAE 14TH JOINT PROPULSION CONFERENCE*, 1978.

[11] M. A. R. Nascimento, *The Selective Bleed Variable Cycle Engine,* 1992.

[12] S. C. Kuo, J. D. Doernbach, G. Champagne, A. Tatara, H. Futamura, Y. Watanabe and T. Aoki, "A Scoping Study for Hypersonic Transport Propulsion Systems," in *International Gas Turbine and Aeroengine Congress and Exposition*, 1992.

[13] D. H. Petley and S. C. Jones, "Thermal management for a Mach 5 cruise aircraft using endothermic fuel," *Journal of Aircraft,* vol. 29, no. 3, pp. 384-389, 1992.

[14] B. W. Sanders and L. J. Weir, "CR-2008-215214: Aerodynamic Design of a Dual-Flow Mach 7 Hypersonic Inlet System for a Turbine-Based Combined-Cycle Hypersonic Propulsion System," NASA, 2008.

[15] Lockheed Martin Corporation, Lockheed SR-71A Blackbird Flight Manual, 1989.

[16] C. E. Kepler and G. A. Champagne, "NASA CR-182202: Supersonic Through-Flow Fan Assessment," NASA, 1988.

[17] R. F. Bergholz and B. D. Hitch, “Thermal Management Systems for High Mach Airbreathing Propulsion,” in *30th Aerospaces Sciences Meeting & Exhibit*, Reno, NV, 1992.

[18] M. Chen, H. Tang, K. Zhang, O. Hui and Y. Wang, “Turbine-based combined cycle propulsion system integration concept design,” *Proc. IMechE Part G: J Aerospace Engineering,* vol. 227, no. 7, pp. 1068-1089, 2012.

[19] F. Guo, M. Liu, G. He, J. Zhou, J. Zhu and Y. You, “Analysis and Suppression of Thrust Trap for Turbo-Ramjet Mode Transition with the Integrated Optimal Control Method,” *Aerospace,* vol. 10, no. 667, 2023.

[20] ESDU, “90012: ENERGY HEIGHT METHOD FOR FLIGHT PATH OPTIMISATION,” Engineering Sciences Data Unit, 1990.

[21] ESDU, “91016: ENERGY HEIGHT METHOD FOR FLIGHT PATH OPTIMISATION. Addendum A: Numerical method suitable for rapid use on IBM PC compatible computers,” Engineering Services Data Unit, 1991.

[22] Jane's Group UK Ltd, “General Electric J85,” 2021. [Online]. Available: https://customer.janes.com/display/JAE_0300-JAE_.

[23] Jane's Group UK Ltd, “General Electric J79,” 2020. [Online]. Available: https://customer.janes.com/display/JAE_0299-JAE_.

[24] Jane's Group UK Ltd, “[ARCHIVED] Pratt & Whitney J58,” 2009. [Online]. Available: https://customer.janes.com/display/jae_0328-jae_.

[25] N. P. Matthews, R. Seppey, S. A. Prince and Z. A. Rana, “The Application of Rapid Aerodynamic Prediction Techniques to Supersonic Aircraft,” in *AIAA Science and Technology Forum and Exposition*, 2025.

[26] International Standards Organisation (ISO), “ISO 2533:1975 - Standard Atmosphere,” ISO, 1975.



https://dspace.org/

# Turbine-based combined cycle design and performance up to Mach 5.0

**Ashford, Zoe; Pachidis, Vassilios; Prince, Simon A.**

**2026-01-12**
American Institute of Aeronautics and Astronautics (AIAA)
https://doi.org/10.2514/6.2026-1189
Ashford Z, Pachidis V, Prince SA. (2026) Turbine-based combined cycle design and performance up to Mach 5.0. In: AIAA SCITECH 2026 Forum, 12-16 January 2026, Orlando, Florida, Article number 2026-1189

Downloaded from a DSpace repository. https://dspace.org/